

# Rotational spectrum of $^{13}\text{C}_2$ -methyl formate ( $\text{HCOO}^{13}\text{CH}_3$ ) and detection of the two $^{13}\text{C}$ -methyl formate in Orion<sup>★</sup>

M. Carvajal<sup>1</sup>, L. Margulès<sup>2</sup>, B. Tercero<sup>3</sup>, K. Demyk<sup>4</sup>, I. Kleiner<sup>5</sup>, J. C. Guillemin<sup>6</sup>, V. Lattanzi<sup>4</sup>, A. Walters<sup>4</sup>, J. Demaison<sup>2</sup>, G. Wlodarczak<sup>2</sup>, T. R. Huet<sup>2</sup>, H. Møllendal<sup>7</sup>, V. V. Ilyushin<sup>8</sup>, and J. Cernicharo<sup>3</sup>

<sup>1</sup> Departamento de Física Aplicada, Facultad de Ciencias Experimentales, Universidad de Huelva, 21071 Huelva, Spain  
e-mail: miguel.carvajal@dfa.uhu.es

<sup>2</sup> Laboratoire de Physique des Lasers, Atomes, et Molécules, UMR CNRS 8523, Université de Lille I, 59655 Villeneuve d'Ascq Cedex, France

<sup>3</sup> Laboratory of Molecular Astrophysics, CAB-CSIC, INTA. Ctra. de Torrejón a Ajalvir, km 4, 28850 Torrejón de Ardoz, Madrid, Spain

<sup>4</sup> Centre d'Étude Spatiale des Rayonnements, Université de Toulouse (UPS), CNRS, UMR 5187, 9 avenue du Colonel Roche, BP 44346, 31028 Toulouse, Cedex 4, France

<sup>5</sup> Laboratoire Interuniversitaire des Systèmes Atmosphériques, UMR CNRS 7583, Université Paris 7 et Université Paris 12, 61 Av. Charles de Gaulle, 94010 Créteil Cedex, France

<sup>6</sup> Sciences Chimiques de Rennes - École Nationale Supérieure de Chimie de Rennes - CNRS, 35708 Rennes Cedex 7, France

<sup>7</sup> Centre for Theoretical and Computational Chemistry (CTCC), Department of Chemistry, University of Oslo, PO Box 1033 Blindern, 0315 Oslo, Norway

<sup>8</sup> Institute of Radio Astronomy of NASU, Krasnoznamennaya 4, 61002 Kharkov, Ukraine

Received 1 December 2008 / Accepted 2 March 2009

## ABSTRACT

**Context.** Laboratory measurements and analysis of the microwave and millimeter-wave spectra of potential interstellar molecules are a prerequisite for their subsequent identification by radioastronomical techniques. The spectral analysis provides spectroscopic parameters that are used in the assignment procedure of the laboratory spectra, and that also predict the frequencies of transitions not measured in the laboratory with a high degree of precision.

**Aims.** An experimental laboratory study and its theoretical analysis is presented for  $^{13}\text{C}_2$ -methyl formate ( $\text{HCOO}^{13}\text{CH}_3$ ) allowing a search for this isotopologue in the Orion molecular cloud. The  $^{13}\text{C}_1$ -methyl formate ( $\text{H}^{13}\text{COOCH}_3$ ) molecule was also searched for in this interstellar cloud, using previously published spectroscopic data.

**Methods.** The experimental spectra of  $^{13}\text{C}_2$ -methyl formate were recorded in the microwave and sub-mm energy ranges (4–20 GHz, 8–80 GHz, 150–700 GHz). The spectra were analyzed using the Rho-Axis Method (RAM), which takes the  $\text{CH}_3$  internal rotation and the coupling between internal rotation and global rotation into account.

**Results.** Twenty-seven spectroscopic constants of  $^{13}\text{C}_2$ -methyl formate have been obtained from a fit of 936 transitions of the ground torsional state with a standard (unitless) deviation of 1.08. A prediction of line positions and intensities is also produced. This prediction allowed us to identify 230  $^{13}\text{C}_2$ -methyl formate lines in the Orion interstellar molecular cloud. We refitted all previously published ground state transitions of the  $^{13}\text{C}_1$ -methyl formate molecule in order to provide a prediction of its ground state spectrum. 234 lines of  $^{13}\text{C}_1$ -methyl formate were detected in the Orion interstellar cloud using that prediction.

**Key words.** line: identification – methods: data analysis – methods: laboratory – methods: observational – ISM: molecules – submillimeter

## 1. Introduction

Since the middle of the 20th century, many spectroscopic studies on methyl formate  $\text{HCOOCH}_3$  have been carried out because of its astrophysical importance. Methyl formate is indeed one of the most abundant organic molecules in interstellar hot cores. Its column density is about  $10^{15}$ – $10^{17}$   $\text{cm}^{-2}$  depending on the objects (e.g. Ikeda et al. 2001; Remijan et al. 2004). It has also been detected in low-mass star-forming regions (hot corinos), such as NGC1333-IRAS4B and IRAS 2A (Bottinelli et al. 2004, 2007). Its large abundance is difficult to account

for with a production mechanism based only on gas phase reactions with methanol (Horn et al. 2004) and grain chemistry should be involved in methyl formate formation. In 1959 Curl studied the chemical structure and the microwave spectrum of the parent methyl formate and 8 other isotopologues (Curl 1959). In 1975 the parent molecule was detected for the first time in the interstellar medium by Brown et al. (1975) and Churchwell et al. (1975). Since this discovery, approximately 900 lines of the ground torsional state have been detected in different interstellar molecular clouds, Sgr B2, Orion KL, and W51 e1/e2 (Lovas 2004). Recently torsionally excited lines of methyl formate have also been observed in Orion KL by Kobayashi et al. (2007) and in W51 e2 by Demyk et al. (2008). It has to be emphasized that such a large number of transitions of methyl formate could only

<sup>★</sup> Tables A.1–A.5 are only available in electronic form at the CDS via anonymous ftp to cdsarc.u-strasbg.fr (130.79.128.5) or via <http://cdsweb.u-strasbg.fr/cgi-bin/qcat?J/A+A/500/1109>

be identified in the interstellar medium thanks to a huge effort in the laboratory.

Millimeter and sub-millimeter wave spectra have been recorded in the laboratory and analyzed in different spectral ranges for the main species  $\text{H}^{12}\text{COO}^{12}\text{CH}_3$ . Chronologically the measurements carried out for the ground torsional state ( $v_t = 0$ ) were performed in the spectral range 8–58 GHz (Bauder 1979), 150–313 GHz (Demaison et al. 1983), 216–506 GHz (Plummer et al. 1984), 200–352 GHz (Plummer et al. 1986), 250–510 GHz (Oesterling et al. 1999), 7–200 GHz (Karakawa et al. 2001), 567–669 GHz (Carvajal et al. 2007), and 110–380 GHz (Maeda et al. 2008a). In 2003 and 2004, a number of transitions were analyzed for the first time in the first excited torsional state  $v_t = 1$  (Odashima et al. 2003; Ogata et al. 2004). In 2007, 4270 transition lines covering the spectral range up to 669 GHz (with  $J_{\text{max}} = 62$ ,  $K_{\text{max}} = 22$  for  $v_t = 0$ ; and  $J_{\text{max}} = 18$ ,  $K_{\text{max}} = 7$  for  $v_t = 1$ ) were globally analyzed using the RAM or Rho-Axis Method (Lin & Swalen 1959; Herbst et al. 1984; Hougen et al. 1994). This global fit of the A- and E-species required 49 parameters to achieve root-mean-square deviations of 94 kHz and 84 kHz corresponding to 3486 and 774 transitions in the ground and first excited torsional states, respectively (Carvajal et al. 2007). The number of lines measured in the ground torsional state  $v_t = 0$  of normal methyl formate has increased very recently by measurements performed using the Fast Scan Submillimeter Spectroscopic Technique (FASSST) and 5366 lines in  $v_t = 0$  were fitted up to 510 GHz (Maeda et al. 2008a). Last year the same authors (Maeda et al. 2008b) also assigned a number of new transitions belonging to the  $v_t = 1$  torsional state of the normal species, and for the first time some 213 transitions belonging to the second excited state  $v_t = 2$ .

In spite of the large quantity of spectroscopic data provided for the main species, there is much less information for the other isotopologues. Curl (1959) reported a few tens of a-type and b-type transitions for  $\text{DCOOCH}_3$ ,  $\text{sym-HCOOCH}_2\text{D}$ ,  $\text{asym-HCOOCH}_2\text{D}$ ,  $\text{HCOOCD}_3$ ,  $\text{H}^{13}\text{COOCH}_3$ ,  $\text{HCOO}^{13}\text{CH}_3$ ,  $\text{HC}^{18}\text{OCH}_3$ , and  $\text{HCO}^{18}\text{OCH}_3$ . In 1995 Oesterling et al. (1995) provided around 900 lines of the spectrum of symmetric monodeuterated methyl formate ( $\text{DCOOCH}_3$ ) in the ground state. In 2006 around 500 measurements for  $^{13}\text{C}_1$  methyl formate,  $\text{H}^{13}\text{COOCH}_3$ , were carried out in the 7–62 GHz, 300–322 GHz and 570–610 GHz spectral range by Willaert et al. (2006). Very recently, the spectrum of  $\text{H}^{13}\text{COOCH}_3$  was also recorded between 110 and 377 GHz using the FASSST spectrometer and more than 4900 transitions belonging to  $v_t = 0$ , 910 transitions belonging to  $v_t = 1$  and 231 transitions belonging to  $v_t = 2$  (Maeda et al. 2008a,b) were fitted separately using the ErHam procedure in the principal axis system (Groner 1992, 1997; Groner et al. 1998). Lately new spectroscopic measurements of monodeuterated species  $\text{HCOOCH}_2\text{D}$  were carried out by Margules et al. (2009). Finally, besides the spectroscopic studies mentioned above, the molecular structure of the main isotopologue of methyl formate has been determined from ab initio calculations (Uchimaru et al. 2003; Senent et al. 2005), which confirmed the experimental values already obtained for the torsional and rotational parameters.

This huge effort of gathering spectroscopic data continues to be pursued in order to prepare the future large sub-millimeter facilities like the ground-based ALMA (Atacama Large Millimeter Array) and the Herschel space observatory. It is expected that these instruments, combined with very precise spectroscopic analysis, will provide accurate information about the formation of stars in interstellar molecular clouds.

The astrophysical study of other molecular isotopologues of methyl formate is important for several reasons. First it gives access to the isotopic abundance in astronomical environments. Second it allows astronomers to identify lines due to the isotopologues in their surveys and hence to eliminate them in order to search for new species. The upcoming ALMA and Herschel sub-mm facilities will provide large amounts of high-precision ( $\Delta\nu \leq 1$  MHz) spectroscopic data in the wavelength range down to  $150 \mu\text{m}$  (corresponding to 2 THz in frequency). The international interferometer ALMA, in addition, will provide an unprecedented spatial resolution and a sensitivity which reaches the limit of line confusion. Many scientific programs for both HIFI/Herschel and ALMA focus on dense clouds with young stars and surrounding material that contain molecular species with numerous and strong transitions throughout the whole sub-mm region. Much of the line emission comes from known species, such as methyl formate and similarly complex molecules. Without spectral identifications, however, the resulting forest of spectral lines will seriously hinder the detection and analysis of new molecular and radical species. This problem is known as the “Weeds and Grass problem”. For an optimal science exploitation of ALMA and Herschel, it is necessary to cut down the weeds and to recognize the grass. Methyl formate and its isotopologues are classified as “class I weed” species due to their abundance in observations. Third, the observation of transitions of isotopologues is needed to derive correct column densities for abundant molecules exhibiting optically thick lines, which could be the case for methyl formate in some hot cores.

We measured the microwave and sub-millimeter wave spectra experimentally for the  $^{13}\text{C}_2$  species of methyl formate in its ground torsional state. To our knowledge, there has been no rotational study for this species since Curl in 1959. The A- and E-symmetry transitions were analyzed together using the RAM model. In addition we also refitted all published experimental ground state transition lines of  $^{13}\text{C}_1$ -methyl formate in order to predict the frequencies and intensities of its ground state spectrum.

The structure of the paper is the following: the experimental details of the recording of the molecular spectra of  $\text{HCOO}^{13}\text{CH}_3$  in the laboratory are given in Sect. 2 and analysis of the spectrum and the resulting spectroscopic parameters are presented in Sect. 3 with a discussion in Sect. 4. In Sect. 5 the astronomical observation of Orion is presented and in Sect. 6 identification of the emission lines used in the astronomical detection of  $^{13}\text{C}_2$ -methyl formate  $\text{HCOO}^{13}\text{CH}_3$  (using the present spectroscopic analysis) and the lines used for detecting  $^{13}\text{C}_1$ -methyl formate  $\text{H}^{13}\text{COOCH}_3$  (using a prediction based on our fit of all published ground state data from the literature) are shown.

## 2. Experiments

### 2.1. Formic acid, methyl- $^{13}\text{C}$ ester ( $^{13}\text{C}_2$ methyl formate) synthesis

Formic acid and sulfuric acid (reagent grade, 95–98%) were purchased from Aldrich. Methanol- $^{13}\text{C}$  was purchased from Cambridge Isotope Laboratories, Inc. Formic acid (2.0 g, 43.5 mmol) and methanol- $^{13}\text{C}$  (1.0 g, 30.3 mmol) were introduced into a one necked cell equipped with a stirring bar and a stopcock. The solution was cooled to around  $-80^\circ\text{C}$  and sulfuric acid (0.3 g, 3.0 mmol) added. The bottom of the cell was then immersed in a liquid nitrogen bath and the gaseous phase removed in vacuo. The stopcock was closed and the solution

was heated up to 40 °C and stirred overnight at this temperature. The cell was then fitted to a vacuum line equipped with two traps. The solution was distilled. High boiling compounds were trapped in the first trap immersed in a bath cooled at  $-70\text{ °C}$  and  $^{13}\text{C}_2$ -methyl formate (1.80 g, 29.5 mmol) was condensed in the second trap immersed in a liquid nitrogen bath ( $-196\text{ °C}$ ). Yield was 97% (based on methanol), and identification by NMR spectroscopy:  $^1\text{H}$  NMR ( $\text{CDCl}_3$ , 400 MHz)  $\delta$  3.68 (dd, 3H,  $^1J_{\text{CH}} = 147.5\text{ Hz}$ ,  $^4J_{\text{HH}} = 0.9\text{ Hz}$ ,  $\text{CH}_3$ ); 8.01 (dq, 1H,  $^3J_{\text{CH}} = 4.2\text{ Hz}$ ,  $^4J_{\text{HH}} = 0.9\text{ Hz}$ , CH).  $^{13}\text{C}$  NMR ( $\text{CDCl}_3$ , 100 MHz)  $\delta$  50.4 ( $\text{CH}_3$ ), 161.1 (d,  $^2J_{\text{CC}} = 2.9\text{ Hz}$ ).

## 2.2. Spectroscopic details

Rotational spectra in the 4–20 GHz spectral range were recorded using a molecular beam microwave Fourier transform spectrometer. A gas mixture of 20 mbar of methyl formate completed with neon as carrier gas to a total pressure of 1.5 bar was prepared. Gas pulses were then expanded into the vacuum tank through a pulsed nozzle to create a supersonic beam. As the nozzle is inserted in the center of the fixed mirror of the Fabry-Perot cavity, the supersonic expansion is parallel to the optical axis of the cavity. Each transition is divided into two Doppler components. Each molecular transition was recorded at high frequency resolution. The central frequencies of the lines were determined by averaging the frequencies of the two Doppler components after transformation of the 4096 data points time domain signal, leading to a resolution of 2.4 kHz in the spectrum. The accuracy of frequency measurements was estimated to be better than 3 kHz. The linewidth for a typical, well-resolved line was 10 kHz.

The rotational spectrum was studied in the 8–80 GHz range using the Oslo Stark spectrometer described briefly in Møllendal et al. (2005) and Møllendal et al. (2006). The accuracy of the spectral measurements is about 0.1 MHz for isolated lines, but some lines are overlapped by much stronger ground state lines.

The millimeter wave measurements were performed in Lille with a source-modulated spectrometer using phase-stabilized backwardwave oscillators working in the frequency range 150–700 GHz, with transitions measured between 150–245 GHz, 320–350 GHz, 510–525 GHz, and 580–661 GHz (Willaert et al. 2006). The pressure in the absorption cell was about 30 mTorr. The linewidth of the lines was Doppler limited. The accuracy of the measurements is about 30 kHz for most lines, at least when they are isolated.

## 3. Analysis of the $\text{HCOO}^{13}\text{CH}_3$ spectrum

### 3.1. Theoretical model

To carry on the analysis we used the so-called “RAM” (“Rho Axis Method”) internal rotation Hamiltonian and a model extended to include perturbation terms through eighth order (Herbst et al. 1984; Hougen et al. 1994). This model is based on the work of Lin & Swalen (1959), Kirtman (1962), and Lees & Baker (1968). This formalism and our code<sup>1</sup> have been completely described in previous studies and applied with success to a number of internal rotor molecules observed in the interstellar medium, i.e. for acetaldehyde,  $\text{CH}_3\text{CHO}$  (Kleiner et al. 1996a),

acetamide  $\text{CH}_3\text{CONH}_2$  (Hollis et al. 2006), and acetic acid  $\text{CH}_3\text{COOH}$  (Ilyushin et al. 2008). All details about this method can be found in those references and therefore will not be described again here. In our “global” approach we fit both A- and E-symmetry transition lines simultaneously. The “bath” of torsional levels involving the states  $\nu_t = 0, 1, 2, \dots$  (up a truncation limit of  $\nu_t = 8$  carefully tested) and the interactions within those torsion-rotation energy levels are also included in the rotation-torsion Hamiltonian matrix elements (Kleiner et al. 1996b). The various terms we are using in the Hamiltonian for the fit of the  $^{13}\text{C}_2$ - (and also for  $^{13}\text{C}_1$ )-methyl formate species, rotational terms, internal rotation terms, and the coupling between internal rotation and global rotation have been described before for normal methyl formate (Carvajal et al. 2007).

### 3.2. Assignments and fit

The present analysis was started by fitting only the rotational parameters  $A$ ,  $B$ ,  $C$ , and  $D_{\text{ab}}$  (used in the RAM non principal axis system), the potential barrier hindering the internal rotation  $V_3$  and  $\rho$ , the coupling term between the internal rotation angular momentum  $P_\gamma$ , and the global rotation angular momentum along the  $z$  molecular axis,  $J_z$ . The internal rotation constant  $F$  was kept fixed to the ab initio value calculated in the equilibrium structure at the CCSD(T)/cc-pV5Z + core correction level of theory. After fitting transitions corresponding to low  $J$  values, we then gradually included transitions with higher  $J$  values.

The principal characteristics exhibited by the  $^{13}\text{C}_2$ -methyl formate spectrum are the same as for the normal species, i.e. a very dense spectrum due to a relatively small  $A$  rotational constant leading to the observation of transitions involving  $J$  values up to 63. The existence of both a-type and b-type transitions and the presence of small amplitude vibrational modes at low frequency leading to the observation of transitions within those levels populated at room temperature also contribute to increasing the number of observed lines in the spectrum. Finally, the spectrum of this species is highly complicated by relatively large internal rotation splittings.

For  $^{13}\text{C}_2$ -methyl formate, a total of 936 A- and E-symmetry transition lines for the ground torsional state were fit using 27 parameters (and fixing the  $F$  parameter) in the following frequency ranges: 4–20 GHz (FTMW spectrometer in Lille), 8–80 GHz (Oslo Stark Spectrometer) 150–245 GHz, 320–350 GHz, 510–525 GHz, and 580–661 GHz (Lille BWO Spectrometer). The maximum value of  $J$  and  $K_a$  included in our fit are 63 and 34, respectively. The 454 lines corresponding to A-symmetry and 482 corresponding to E-symmetry were fitted with root-mean-square deviations of 100.5 kHz and 93.7 kHz, respectively. The 27 transitions measured using the FTMW spectrometer were given a weight in the fit reciprocal to the square of half the linewidth, i.e. 5 kHz, the 582 unblended transitions originating from the millimeterwave measurements in Lille were weighted according to their measurement accuracy of 30 kHz, whereas 31 and 45 blended transitions were assigned experimental errors of 100 and 200 kHz, respectively, according to the broadening of the line. The 223 unblended and the 28 blended transitions from the Oslo Stark spectrometer were weighted 150 kHz and 200 kHz, respectively. The overall quality of the fit is shown in Table 1, which gives the root-mean-square deviations for transitions according to their measurement uncertainties. The global unitless standard deviation of the fit is 1.08 (equivalent to 97.0 kHz of standard deviation), close to experimental accuracy. It is, however, clear that some blended lines show observed-calculated values with high residuals.

<sup>1</sup> The source code for the fit, an example of input data file and a readme file are available on the web site <http://www.ifpan.edu.pl/~kisiel/introt/introt.htm#belgi> managed by Dr. Zbigniew Kisiel. Extended versions of code are also available with one of the authors (I. Kleiner).



**Table 1.** Root-mean-square (rms) deviations from the global fit<sup>a</sup> of transitions involving  $v_t = 0$  torsional energy levels of  $^{13}\text{C}_2$ -methyl formate ( $\text{HCOO}^{13}\text{CH}_3$ ).

		Number of parameters	27		
		Number of lines	936		
		rms of the 936 MW $v_t = 0$ –0 lines	0.0970 MHz		
		rms of the 454 A symmetry lines	0.1005 MHz		
		rms of the 482 E symmetry lines	0.0937 MHz		
Source <sup>b</sup>	Range <sup>c</sup> (GHz)	$J_{\max}, K_{\max}^d$	Number of lines <sup>e</sup>	Uncertainties <sup>f</sup> (MHz)	rms <sup>g</sup> (MHz)
Lille FTMW	4–20	7, 3	27	0.005	0.0067
Lille BWO	150–700 <sup>j</sup>	63, 31	582	0.030	0.0335
Lille BWO	150–700 <sup>j</sup>	58, 29	31	0.100 <sup>h</sup>	0.0705
Oslo Stark	8–80	33, 11	223	0.150 <sup>i</sup>	
Spectr.		28, 7	28	0.200 <sup>i</sup>	0.1644
Lille BWO	150–700 <sup>j</sup>	58, 34	45	0.200 <sup>h</sup>	

<sup>a</sup> Parameter values are given in Table 2. The complete list of observed minus calculated residuals of  $v_t = 0$  lines are given in Supplementary Table A.1. <sup>b</sup> Sources of data: data come from the present work, the different instruments are described in Sect. 2.2. <sup>c</sup> Spectral range of the measurements. <sup>d</sup> Maximum  $J$  and  $K_a$  for each group of measurements. <sup>e</sup> Number of MW lines in each uncertainty group. <sup>f</sup> Uncertainty in MHz used in the fit. <sup>g</sup> Root mean square deviation in MHz for each group. <sup>h</sup> The accuracy of spectral measurements for the Lille backwardwave oscillators spectrometer is about 0.030 MHz for isolated lines but some lines are either blended or present a bad S/N ratio and therefore their measurement accuracy is taken as either 0.100 MHz or 0.200 MHz according to the broadening of the experimental line. <sup>i</sup> The accuracy of spectral measurements for the Oslo Stark spectrometer is about 0.100 MHz for isolated lines although they are considered with an experimental error of 0.150 MHz. When the lines are either blended or present a bad S/N ratio, their measurement accuracy is taken as 0.200 MHz. <sup>j</sup> The Lille spectrometer spectral ranges for these measurements are: 150–245 GHz, 320–350 GHz, 510–525 GHz and 580–661 GHz.

Table 2 shows the values for the 28 rotation-torsion parameters (including one fixed parameter,  $F$ ) used in our final fit for  $\text{HCOO}^{13}\text{CH}_3$ , together with the values for the 49 parameters needed in the fit of the normal species  $\text{H}^{12}\text{COO}^{12}\text{CH}_3$  (Carvajal et al. 2007). Even though the data set is very different and is much more extended for the normal species (3496 lines belonging to the ground torsional state  $v_t = 0$  fitted with a standard deviation of 94 kHz and 774 lines belonging to the first excited state  $v_t = 1$  fitted with a standard deviation of 84 kHz), one can see that the low-order parameters ( $n = 2$ ) agree within 5%, except for  $V_3$  which is discussed below. For the normal species of methyl formate, because of the more extended data set involving transitions within the ground  $v_t = 0$  and first excited torsional state  $v_t = 1$ , a number of higher order terms were also determined. In the case of  $^{13}\text{C}_2$ -methyl formate isotopologue, those terms cannot be determined and they were fixed to zero. Also, since we do not have any  $v_t = 1$  transitions included in the fit, the two torsional parameters  $V_3$  (the height of the barrier) and  $F$  (the internal rotation parameter) are highly correlated and cannot be fitted simultaneously. We thus decided to fix the value of the  $F$  parameter to its ab initio value as described above. Finally for  $^{13}\text{C}_2$ -methyl formate isotopologue, the  $V_6$  parameter in the torsional potential  $V(\gamma) = V_3/2(1 - \cos 3\gamma) + V_6/2(1 - \cos 6\gamma) + \dots$  could not be determined either. This  $V_6$  term is rather large for normal methyl formate ( $23.9018(636) \text{ cm}^{-1}$ ) and we expect its value to have the same magnitude for  $^{13}\text{C}_2$ -species. At this stage, since we cannot determine  $V_3$  and  $V_6$  at the same time by fitting lines only from the ground torsional state, we decided to maintain the value of  $V_6$  fixed to zero for the  $^{13}\text{C}$  species of methyl formate. For these reasons, the value of  $V_3$  determined in our present fit can only be considered as an effective value, containing the contribution of  $V_6$ .

The variations of structural parameters and internal rotation parameters upon substitution are presented in Table 3. For the normal species of methyl formate and for  $^{13}\text{C}_2$ -methyl formate we show the values of those parameters obtained from our global fits, after transforming the RAM rotational constants into the PAM constants (following a procedure described in

Carvajal et al. 2007). The angle  $\theta_{\text{RAM}}$  between the RAM axis system and the PAM axis system varies from the normal species ( $24.83^\circ$ ) to  $^{13}\text{C}_2$ -methyl formate ( $23.68^\circ$ ) by 4.6%. The variation of the angle  $\langle(i, a)\rangle$  between the  $\text{C}_3$  symmetry axis of the methyl-top and the a- principal axis between the two species is 2.5%. The internal rotation parameter  $\rho$ , which is the coupling between internal rotation and global rotation varies only by 0.3%. It is clear from the first two columns of Table 3 that the structure does not change much upon substitution by  $^{13}\text{C}$ .

In Table 3, we also present the values obtained by Maeda et al. (2008b) for  $^{13}\text{C}_1$ -methyl formate species, using the ErHam procedure (Groner 1992, 1997; Groner et al. 1998), and the values obtained in this work by a global fit of the available data for the ground torsional state of this species. These 4954 lines were refitted using 24 parameters up to  $J_{\max} = 59$  with a standard deviation of 66.9 kHz. The complete set of fitted parameters in this RAM global fit will be published elsewhere. The global approach provides good agreement between the parameter values of both  $^{13}\text{C}$  methyl formate species. Structural comparisons between the ErHam procedure and the global RAM procedure are, however, difficult to make since the ErHam method fits each torsional state  $v_t$  separately, giving rise to parameters showing a strong dependence on the torsional state.

Supplementary Table A.1 containing all included lines in our fit for  $^{13}\text{C}_2$  methyl formate shows the line assignments, the observed frequencies with the measurement uncertainties (in parentheses), the computed frequencies with the estimated theoretical uncertainties (in parentheses), the observed-calculated values, the line strengths in the  $v_t = 0$  torsional ground state, and the lower state energies relative to the  $J = K_a = 0$  A-species level taken as the zero for energy levels.

### 3.3. Intensity calculations

The intensity calculations for  $\text{HCOO}^{13}\text{CH}_3$  were performed using exactly the same procedure as described for the normal species  $\text{HCOOCH}_3$  by Carvajal et al. (2007) so we do not repeat this procedure here.

**Table 2.** Torsion-rotation parameters needed for the global fit of transitions involving  $u_1 = 0$  and  $u_1 = 1$  torsional energy levels of methyl formate ( $\text{H}^{12}\text{COO}^{12}\text{CH}_3$ ) and torsion-rotation parameters needed for the global fit of transitions involving  $u_1 = 0$   $^{13}\text{C}_2$ -methyl formate ( $\text{HCOO}^{13}\text{CH}_3$ ).

$nlm^d$	Operator <sup>b</sup>	Parameter	$\text{HCOO}^{12}\text{CH}_3$	$\text{HCOO}^{13}\text{CH}_3$	$nlm$	Operator	Parameter	$\text{HCOO}^{12}\text{CH}_3$	$\text{HCOO}^{13}\text{CH}_3$
220	$(1 - \cos 3\gamma)/2$	$V_3$	370.924(113)	407.1549(147) <sup>e</sup>	404	$-P^4$	$D_J$	0.42854(455) $10^{-6}$	0.15312(163) $10^{-6}$
	$P_\gamma^2 P_a$	$F$	5.49038(129)	5.69168218 <sup>e</sup>		$-P^2 P_a^2$	$D_{JK}$	-0.19285(527) $10^{-5}$	0.21223(170) $10^{-5}$
211	$P_\gamma P_a$	$\rho$	0.08427127(723)	0.0845207(106)		$-P^4$	$D_K$	0.36534(594) $10^{-5}$	-0.17369(181) $10^{-5}$
202	$P_a^2$	$A^{\text{RAM}}$	0.5884101(188)	0.5857484(245)		$-2P^2(P_b^2 - P_c^2)$	$\delta_J$	0.17990(227) $10^{-6}$	0.39739(813) $10^{-7}$
	$P_b^2$	$B^{\text{RAM}}$	0.3082455(179)	0.2959971(182)		$-[P_a^2(P_b^2 - P_c^2)]$	$\delta_K$	0.28824(900) $10^{-6}$	0.108794(621) $10^{-5}$
	$P_c^2$	$C^{\text{RAM}}$	0.17711843(416)	0.1729010(134)		$P^2(P_a P_b + P_b P_a)$	$D_{abJ}$	0.0 <sup>f</sup>	0.24287(221) $10^{-6}$
440	$(P_a P_b + P_b P_a)$	$D_{ab}$	-0.1649794(162)	-0.1573691(747)	642	$(P_a^3 P_b + P_b P_a^3)$	$D_{abK}$	0.20747(108) $10^{-5}$	0.13608(491) $10^{-5}$
	$P^4$	$k_4$	0.0004368(184)	0.0 <sup>f</sup>		$(1 - \cos 6\gamma)P^2$	$N_6$	-0.507(127) $10^{-4}$	0.0 <sup>f</sup>
	$(1 - \cos 6\gamma)/2$	$V_6$	23.9018(636)	0.0 <sup>f</sup>		$(1 - \cos 6\gamma)(P_b^2 - P_c^2)$	$c_{11}$	-0.0014751(202)	0.0 <sup>f</sup>
431	$P_\gamma^3 P_a$	$k_3$	-0.00012758(711)	0.0 <sup>f</sup>		$2P^4(P_b^2 - P_c^2)$	$c_3$	0.45962(750) $10^{-6}$	0.0 <sup>f</sup>
422	$P^2 P^2$	$G_v$	0.2709(432) $10^{-5}$	0.4682(101) $10^{-4}$	624	$(1 - \cos 3\gamma)P^4$	$f_6$	0.9957(441) $10^{-7}$	0.0 <sup>f</sup>
	$2P^2(P_b^2 - P_c^2)$	$c_1$	0.000018117(264)	0.0 <sup>f</sup>		$(1 - \cos 3\gamma)(P_b^2 - P_c^2)P^2$	$c_{2J}$	0.5483(445) $10^{-7}$	0.0 <sup>f</sup>
	$\sin 3\gamma(P_a P_c + P_c P_a)$	$D_{ac}$	-0.0068896(540)	-0.0040623(839)		$(1 - \cos 3\gamma)[P_a^2(P_b^2 - P_c^2) - P_c^2]$	$c_{2K}$	0.24458(404) $10^{-6}$	0.0 <sup>f</sup>
	$(1 - \cos 3\gamma)P^2$	$F_v$	-0.0025827(184)	-0.0007557(425)		$2P_\gamma^2(P_b^2 - P_c^2)P^2$	$c_{1J}$	0.17386(211) $10^{-8}$	0.0 <sup>f</sup>
	$(1 - \cos 3\gamma)P_a^2$	$k_5$	0.0112949(386)	0.0124250(566)		$(1 - \cos 3\gamma)(P_a P_b + P_b P_a)P^2$	$d_{abJ}$	-0.12488(883) $10^{-6}$	0.9060(708) $10^{-7}$
	$(1 - \cos 3\gamma)(P_b^2 - P_c^2)$	$c_2$	0.0012608(253)	0.0 <sup>f</sup>		$(1 - \cos 3\gamma)(P_a^3 P_b + P_b P_a^3)$	$d_{abK}$	0.19649(625) $10^{-6}$	0.3349(260) $10^{-6}$
	$(1 - \cos 3\gamma)(P_a P_b + P_b P_a)$	$d_{ab}$	-0.0063031(176)	-0.013852(236)		$(1 - \cos 3\gamma)P^2 P^2$	$k_{5J}$	-0.5853(125) $10^{-6}$	0.0 <sup>f</sup>
	$P^2 P_a^2$	$k_2$	-0.2837(166) $10^{-4}$	0.0 <sup>f</sup>	633	$P_\gamma^2 P_a P_a$	$k_{3J}$	0.7061(198) $10^{-7}$	0.0 <sup>f</sup>
	$P_\gamma^2(P_a P_b + P_b P_a)$	$\Delta_{ab}$	-0.8874(434) $10^{-5}$	-0.16792(565) $10^{-3}$		$P_\gamma^3 P_a^3$	$k_{3K}$	-0.8230(461) $10^{-7}$	0.0 <sup>f</sup>
	$\sin 3\gamma(P_b P_c + P_c P_b)$	$D_{bc}$	0.0 <sup>f</sup>	0.0010563(383)		$P_\gamma^3\{P_{av}(P_b^2 - P_c^2)\}$	$c_{12}$	-0.6946(110) $10^{-7}$	0.0 <sup>f</sup>
413	$P_\gamma P_a P^2$	$L_v$	0.3932(110) $10^{-5}$	-0.2045(247) $10^{-5}$	606	$P_\gamma^3\{P_{av}^2 P_b\}$	$\delta\delta_{ab}$	-0.61998(808) $10^{-7}$	0.0 <sup>f</sup>
	$P_\gamma P_a^3$	$k_1$	-0.00000596(279)	0.0 <sup>f</sup>		$P^6$	$H_J$	0.333(35) $10^{-12}$	-0.31(1) $10^{-13}$
	$P_\gamma\{P_{av}(P_b^2 - P_c^2)\}$	$c_4$	0.1100(561) $10^{-6}$	0.39452(688) $10^{-5}$		$P^4 P_a^2$	$H_{JK}$	0.15998(570) $10^{-10}$	0.0 <sup>f</sup>
	$P_\gamma\{P_{av}^2 P_b\}$	$\delta_{ab}$	-0.10141(145) $10^{-4}$	0.1707(107) $10^{-4}$		$P^2 P_a^4$	$H_{KJ}$	-0.7620(187) $10^{-10}$	0.0 <sup>f</sup>
						$P^6$	$H_K$	0.9098(281) $10^{-10}$	0.0 <sup>f</sup>
						$P^2\{P_{av}^2(P_b^2 - P_c^2)\}$	$h_{JK}$	0.0 <sup>f</sup>	0.1130(25) $10^{-11}$
					826	$(1 - \cos 3\gamma)(P_b^2 - P_c^2)P^4$	$c_{2J}$	0.1746(201) $10^{-11}$	0.0 <sup>f</sup>
					844	$2P_\gamma^2(P_b^2 - P_c^2)P^2$	$c_{3J}$	-0.29116(514) $10^{-10}$	0.0 <sup>f</sup>

<sup>a</sup> Notation from Ilyushin et al. (2003);  $n = l + m$ , where  $n$  is the total order of the operator,  $l$  is the order of the torsional part and  $m$  is the order of the rotational part. <sup>b</sup> Notation from Ilyushin et al. (2003).  $\{A, B\} = AB + BA$ . The product of the parameter and operator from a given row yields the term actually used in the vibration-rotation-torsion Hamiltonian, except for  $F, \rho$  and  $A$ , which occur in the Hamiltonian in the form  $F(P_\gamma - \rho P_a)^2 + A^{\text{RAM}} P_a^2$ . <sup>c</sup> Values of the parameters in  $\text{cm}^{-1}$ , except for  $\rho$  which is unitless, for the normal species from a fit of  $u_1 = 0$  and  $u_1 = 1$  data (from Carvajal et al. 2007). The 3496 MW lines from  $u_1 = 0$  fit with a standard deviation of 94 kHz and the 774 MW lines from  $u_1 = 1$  fit with a standard deviation of 84 kHz. <sup>d</sup> Values of the parameters from the present fit for the ground torsional state  $u_1 = 0$  of  $^{13}\text{C}_2$  methyl formate. All values are in  $\text{cm}^{-1}$ , except for  $\rho$  which is unitless. Statistical uncertainties are given in parentheses in units of the last quoted digit. <sup>e</sup> The internal rotation constant  $F$  of  $^{13}\text{C}_2$  methyl formate was kept fixed to the ab initio value calculated in the equilibrium structure (see Sect. 3.2). <sup>f</sup> Kept fixed. <sup>g</sup> Effective value, see text.

**Table 3.** Rotational constants in the principal axis system (PAM), angles between the principal axis and the methyl top axis and internal rotation parameters upon isotopic substitution.

	$\text{HCOOCH}_3^a$	$\text{HCOO}^{13}\text{CH}_3^b$	$\text{H}^{13}\text{COOCH}_3^c$	$\text{H}^{13}\text{COOCH}_3^d$	$\text{H}^{13}\text{COOCH}_3^d$	$\text{H}^{13}\text{COOCH}_3^d$
	Global fit ( $v_t = 0, 1$ )	Global Fit ( $v_t = 0$ )	Global Fit ( $v_t = 0$ )	$v_t = 0$	$v_t = 1$	$v_t = 2$
$A$ (MHz)	19928.890(602)	19629.65(176)	19709.546(258)	19798.73249(43)	19917.3706(78)	20034.7(47)
$B$ (MHz)	6952.169(585)	6804.42(171)	6909.555(225)	6864.74991(14)	6798.41624(91)	6748.99(76)
$C$ (MHz)	5309.877(125)	5183.442(402)	5274.5475(189)	5262.53086(13)	5236.59430(30)	5213.360(21)
$\langle i, a \rangle^e$	52.97	51.68	52.48			
$\theta_{\text{RAM}}^f$	24.83	23.68	24.54	21.8604(79)	22.201(11)	22.867(34)
$\rho$	0.08427127(723)	0.0845207(106)	0.08407138(395)	0.084497(20)	0.086209(43)	0.08426(14)
$F$ ( $\text{cm}^{-1}$ )	5.49038(129)	5.69168218 <sup>g</sup>	5.8039485 <sup>g</sup>	5.954(1)	5.7704(3)	5.802(1)
$\sigma^h$	1.43	1.08	0.67	0.86	0.99	1.07
$N^o$ of transitions	4270	936	4954	4921	910	231

<sup>a</sup> Rotation-torsion parameters for the normal species  $\text{HCOOCH}_3$  obtained in our work in the RAM-axis system, after transforming the RAM values for the  $A$ ,  $B$ ,  $C$  rotational parameters into PAM values following the procedure described in Carvajal et al. (2007). Note that Maeda et al. (2008a) also presents a fit for the normal species (but not including the same data set), using the ErHam procedure and fitting separately 5366 lines, 1228 lines and 213 lines belonging to  $v_t = 0, 1$  and 2 with unitless standard deviations of 1.11, 1.18 and 0.81 respectively. Accuracy of their line measurements is about 100 kHz. <sup>b</sup> Rotation-torsion parameters for  $^{13}\text{C}_2$ -methyl formate from the present work transformed to the Principal Axis System. <sup>c</sup> Rotation-torsion parameters for  $^{13}\text{C}_1$ -methyl formate from the present work transformed to the Principal Axis System. The parameters were obtained with RAM model from a fit of all  $v_t = 0$  data presently available (4954 lines with 24 fitted parameters) in the literature and will be published soon. <sup>d</sup> Rotation-torsion parameters for  $^{13}\text{C}_1$ -methyl formate from Maeda et al. (2008b) obtained separately for each torsional state studied, using the ErHam procedure. <sup>e</sup> Angle in degrees between the a-principal axis and the methyl top axis ( $i$ ). <sup>f</sup> The angle  $\theta_{\text{RAM}}$  between the a-principal axis and the a-RAM axis is given in degrees and obtained from Eq. (1) from Carvajal et al. (2007), with the parameters  $A^{\text{RAM}}$ ,  $B^{\text{RAM}}$ ,  $C^{\text{RAM}}$ , and  $D_{\text{ab}}$  of Table 2. <sup>g</sup> Fixed to the ab initio value. <sup>h</sup> Unitless standard deviation.

For  $\text{HCOO}^{13}\text{CH}_3$ , we assume that the electric dipole moment components are the same as for the normal species, i.e.  $\mu_a = +1.63$  D and  $\mu_b = +0.68$  D in the principal axis system (Bauder 1979). We adopt the same *chemical* convention for the signs of the dipole moments as we did for the normal species; i.e.,  $\mu_a$  and  $\mu_b$  have positive signs with respect to the chosen principal axes (the dipole moment points from the positive to the negative charges of the molecule). For  $\text{HCOO}^{13}\text{CH}_3$ , the RAM dipole moment components obtained by Eq. (2) of Carvajal et al. (2007), using a value of  $\theta_{\text{RAM}}$  between the RAM axis system and the PAM axis system of  $23.68^\circ$  are 1.766 and  $-0.032$  Debye for  $\mu_a$  and  $\mu_b$ , respectively. For  $\text{H}^{13}\text{COOCH}_3$ , the RAM a- and b-dipole moment components are 1.765 D and  $-0.058$  D, respectively, and the value of  $\theta_{\text{RAM}}$  is  $24.54^\circ$ . It is important to note that the precision of the line strengths depends on the dipole moment components that have been determined so far by Stark experiments only for the normal species of methyl formate and not for any of the  $^{13}\text{C}$  species. For these reasons, we estimate the uncertainties on the line strengths to be less than a few % for the strong lines (typically a-type transitions) and up to 10% for the weaker lines (typically b-type transitions).

The line strengths are presented in Table A.1 of the supplementary material. A more complete list of line frequencies and line strengths have also been predicted for the ground torsional state of  $\text{HCOO}^{13}\text{CH}_3$ . This prediction will be published in the future and is available upon request to the authors (M.C. or I.K.).

#### 4. Discussion

This paper shows that the structural parameters (rotational constants, torsional parameters, angles between the principal axes, and the direction of the methyl group) do not vary much upon isotopic substitution. In view of the very large amount of spectroscopic data that has become available for methyl formate and its isotopologues over the past few years, it is now very important to clarify and to unify this data both experimentally and

theoretically if we want to make it easy to use for astrophysical purposes.

The situation is not completely clarified even for the torsional ground state of the normal species of methyl formate: 5366 lines fit to a root-mean-square deviation of 111 kHz for  $v_t = 0$  using 33 parameters in the ErHam procedure (Maeda et al. 2008a). However, this data does not include the 434 lines measured in 2007 by Carvajal et al. in the 567–669 GHz and corresponding to higher values of  $J$  and  $K_a$  ( $J_{\text{max}} = 62$  and  $K_{\text{max}} = 22$ ). The extension to higher frequency is a challenge for spectroscopists but can be important because some of the new radio-astronomy facilities (Herschel, ALMA, SOFIA) will operate in this spectral range. Some previously measured lines for the normal species of methyl formate also showed discrepancies (Carvajal et al. 2007) and needed to be remeasured using a higher precision instrument. During the course of the present paper remeasurements, as well as new measurements, were underway for  $\text{H}^{12}\text{COO}^{12}\text{CH}_3$  normal methyl formate and a data set containing about 10 000 lines has been included in a global fit using the RAM method (Ilyushin et al. 2009).

Different theoretical approaches have also turned out to be very useful in analyzing the very dense and complex spectra of organic molecules. Complementary to the ErHam approach that fits all torsional states separately (and hence gets as many set of parameters as torsional states, but also avoids the problems of having errors spread out among the various torsional states), the RAM approach can be used to fit all available data simultaneously corresponding to the torsional *bath* levels ( $v_t = 0, 1$ , and 2), not only for the normal species (Ilyushin et al. 2009), but also for the  $^{13}\text{C}_1$ -methyl formate  $\text{H}^{13}\text{COOCH}_3$  isotopologue, for which such data have been published very recently. In addition to decreasing the number of fitted parameters in the global model relative to a separate fit of torsional levels, the RAM method presents the advantage of including terms corresponding to rotation-torsion interactions between different torsional states in the Hamiltonian matrix. Inclusion of torsion-rotation transitions belonging to the excited torsional states  $v_t = 1$  and 2 for

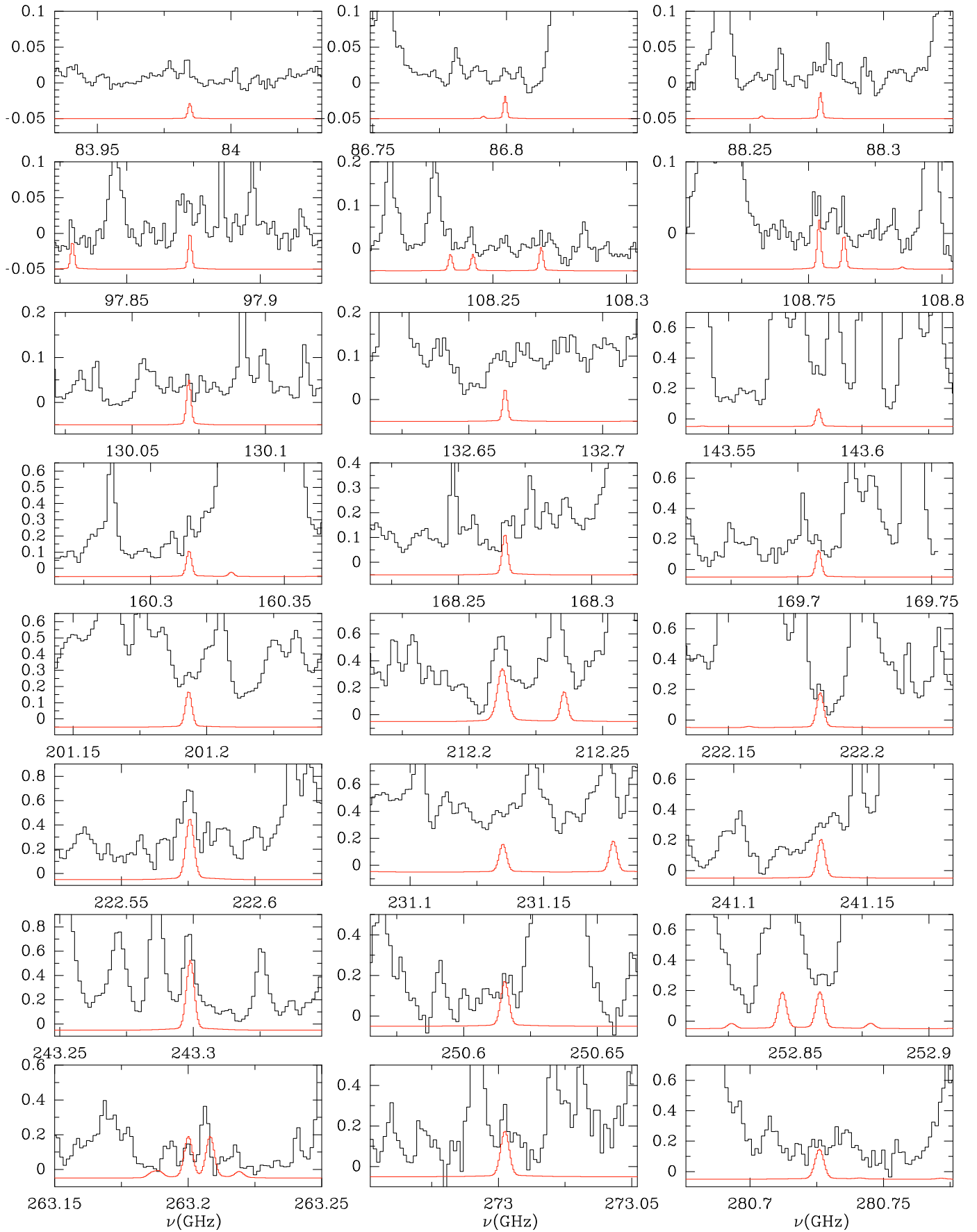


**Fig. 1.**  $\text{HCOO}^{13}\text{CH}_3$  detection in Orion. The spectra in all figures are in units of main beam temperature ( $T_{\text{mb}}$ , K). The histogram spectra are the observations compared to the A- $\text{HCOO}^{13}\text{CH}_3$  model (smooth line).

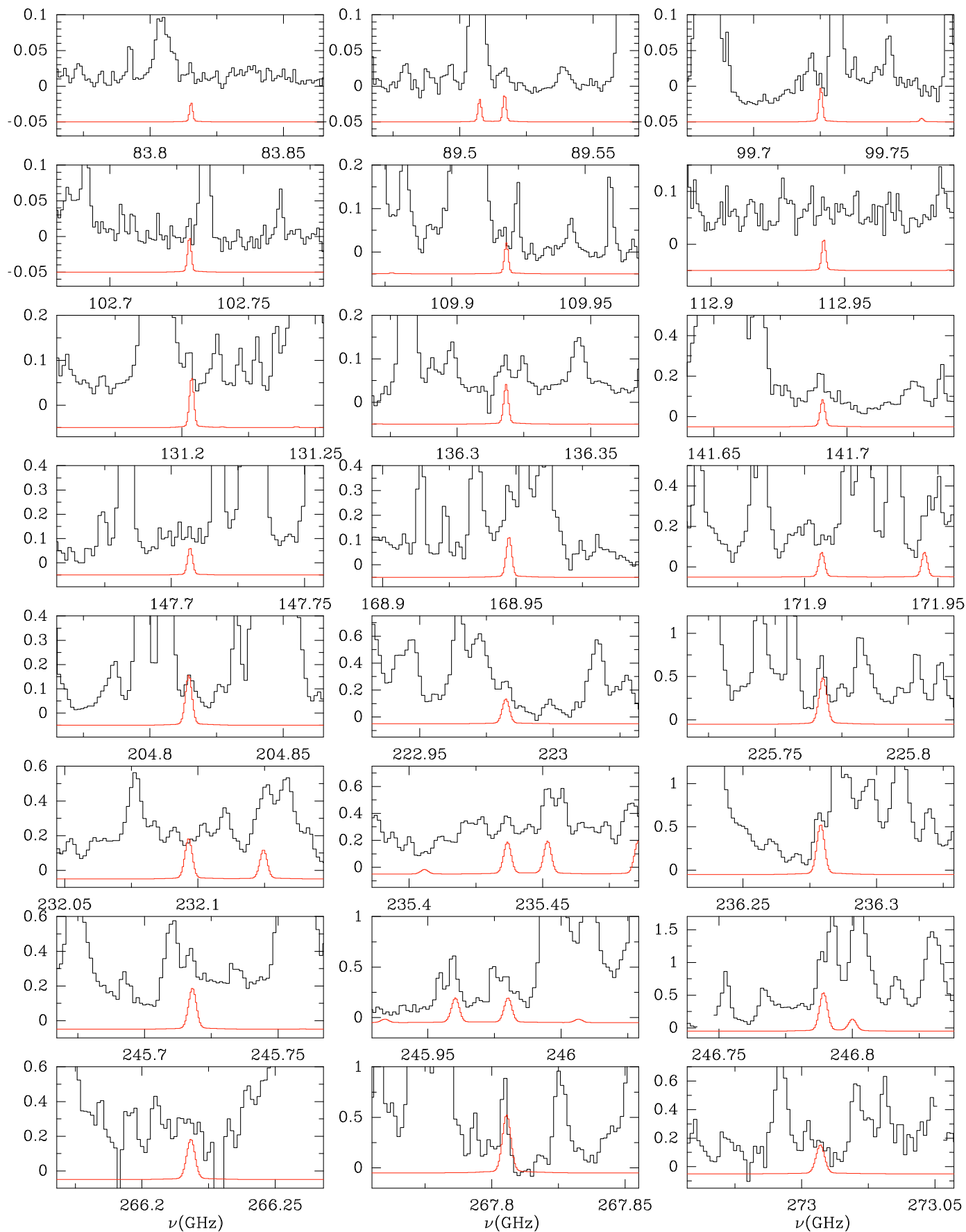


**Fig. 2.**  $\text{H}^{13}\text{COOCH}_3$  detection in Orion. The spectra in all figures are in units of main beam temperature ( $T_{\text{mb}}$ , K). The histogram spectra are the observations compared to the A- $\text{H}^{13}\text{COOCH}_3$  model (smooth line).



the  $^{13}\text{C}$ -methyl formate species is also desirable to help refine the torsional potential barrier.

## 5. Astronomical observation

The observations were carried out using the IRAM 30 m radio telescope during September 2004 (3 mm and 1.3 mm), March 2005 (2 mm) and April 2005 (3 mm and 1.3 mm). We covered the total spectral range allowed by the 30-m receivers. The four SiS receivers operating at 3, 2, and 1.3 mm were used simultaneously. Each receiver was tuned to a single sideband with image rejections within 20–27 dB (3 mm receivers), 12–16 dB (2 mm receivers), and 13 dB (1.3 mm receivers).

System temperatures were 100–350 K for the 3 mm receivers, 200–500 K for the 2 mm receivers, and 200–800 K for the 1.3 mm receivers, depending on the particular frequency, weather conditions, and source elevation. The intensity scale was calibrated using two absorbers at different temperatures and using the Atmospheric Transmission Model (Cernicharo 1985; Pardo et al. 2001).

Pointing and focus were regularly checked on the nearby quasars 0420–014 and 0528+134. The observations were made in the balanced wobbler-switching mode, with a wobbling frequency of 0.5 Hz and a beam throw in azimuth of  $\pm 240''$ . The backends used were two filter banks with  $512 \times 1$  MHz channels and a correlator providing two 512 MHz bandwidths and 1.25 MHz resolution. We performed a spectral line survey for the central frequencies that were chosen systematically: from 80 GHz to 115.5 GHz by 500 MHz for the 3 mm domain; from 130.250 GHz to 176.750 GHz by 500 MHz for the 2 mm; from 197 to 241 by 500 MHz for the 1.3 mm (low frequency); and from 241.250 to 281.750 GHz by 500 MHz for the 1.3 mm domain (high frequency). We pointed toward the (survey) position  $\alpha = 5^{\text{h}}35^{\text{m}}14.5^{\text{s}}$ ,  $\delta = -5^{\circ}22'30.0''$  (J2000.0) corresponding to IRc2. The detailed procedure used for the analysis of the line survey is described in Tercero et al. (in preparation).

## 6. Astronomical modeling

In agreement with previous observations of Orion, four well-defined kinematic regions with quite different physical and chemical conditions (Blake et al. 1987, 1996) are implied by the observed LSR velocities and line widths: (i) the narrow ( $\lesssim 5 \text{ km s}^{-1}$  line width) feature at  $v_{\text{LSR}} \approx 9 \text{ km s}^{-1}$  forming a N-S *extended ridge* or ambient cloud; (ii) a compact and quiescent region, *compact ridge*, ( $v_{\text{LSR}} \approx 7\text{--}8 \text{ km s}^{-1}$ ,  $\Delta v \approx 3 \text{ km s}^{-1}$ ) identified for the first time by Johansson et al. (1984); (iii) the more turbulent and compact *plateau* ( $v_{\text{LSR}} \approx 6\text{--}10 \text{ km s}^{-1}$ ,  $\Delta v \gtrsim 25 \text{ km s}^{-1}$ ); (iv) the *hot core* component ( $v_{\text{LSR}} \approx 3\text{--}5 \text{ km s}^{-1}$ ,  $\Delta v \lesssim 10\text{--}15 \text{ km s}^{-1}$ ) first observed in ammonia emission (Morris et al. 1980). Methyl formate emission comes mainly from the compact ridge component.

To model the emission from the  $^{13}\text{C}$  isotopologues of methyl formate, we added the contribution of each Orion KL component to the line profiles and intensities. We assumed LTE approximation in all the cloud components. The column densities we show are for each state of  $^{13}\text{C}$  methyl formate (A, E). For the compact ridge, a column density of  $7 \times 10^{14} \text{ cm}^{-2}$ , a linewidth of  $4 \text{ km s}^{-1}$ , and a rotational temperature of 110 K are the best parameters for reproducing the bulk of the methyl formate isotopologues emission. A low contribution of the other components is needed to fully reproduce the observations. For the extended ridge, the plateau, and the hot core, we obtained a column density of  $1 \times 10^{13} \text{ cm}^{-2}$  for each one with rotational temperatures of

60, 125, and 225 K, respectively, and the line parameters are the typical values for each component, as given above. For the compact ridge component we assumed a source of  $15''$  diameter with uniform brightness temperature and optical depth over this size, placed  $7''$  from the pointed position (the observation was pointed towards IRc2, while the organic, saturated O-rich species seem to come mainly from the compact ridge). For the extended ridge, the plateau, and the hot core, we assumed a size of 120, 30, and  $10''$ , respectively.

The detailed modeling of methyl formate includes the main isotopologue, the vibrationally excited states, and the detected isotopologues that will be published elsewhere (Tercero et al., in preparation). A first look at the emission lines of the main isotopologue indicates optically thin lines, therefore we expect a column density of  $2 \times 10^{16} \text{ cm}^{-2}$  for each methyl formate state (A and E, assuming a ratio  $^{12}\text{C}/^{13}\text{C} \approx 35$ ).

Figures 1 and 2 show selected observed lines of the  $^{13}\text{C}$  isotopologues (histogram spectra), together with the model results (A state, thin offset curves) in units of  $T_{\text{mb}}$ . The overlap of several molecular lines in Orion mainly affects the intensity of weak lines (it is difficult to provide a good baseline) and our model does not take care of this contribution; nevertheless, the difference between model and observation intensities is always below 20%. Also, the differences between model and observations (in intensity, velocity, and line width) at the frequencies 212.2, 222.6, 243.3 GHz in Fig. 1 and at the frequencies 225.8, 236.3, 246.8, 267.8 GHz in Fig. 2 stem from the observed lines being a mixture of A and E transitions from the  $^{13}\text{C}$  isotopologues, whereas we only show the A state contribution provided by the model. The good agreement found for the other lines shown (intensities differ by less than 20%) allows us to be confident of the detection and of the results of the model.

Tables A.2–A.5 of supplementary material give the model predictions, observed peak intensities and frequencies, and the predicted frequencies from the rotational constants obtained in this paper, for all those lines of these isotopologues that are not strongly blended with other lines. The differences between the intensity of the model and the peak intensity of the observed lines are mostly due to the contribution from many other molecular species (the high overlap with other lines makes it difficult to provide a good baseline for the weak lines of  $^{13}\text{C}$  methyl formate). It is worth noting that the two  $^{13}\text{C}$  isotopologues of methyl formate and four of ethyl cyanide ( $^{13}\text{C}$  and  $^{15}\text{N}$  isotopologues, see Demyk et al. 2007; and Margules et al. 2008) contribute more than 1500 lines in the 80–280 GHz domain covered by the Orion line survey of Tercero et al. (in preparation).

*Acknowledgements.* Part of this work was supported by the Andalusian Government (Spain) project number FQM-3014 and by the French ANR-08-BLAN-0054 TopModel grant. J.-C.G. thanks the CNES for financial support. This work was supported by the French National Programme “Physique et Chimie du Milieu Interstellaire” and by the European Research Training Network “Molecular Universe” (MRTN-CT-2004-512302). Two of us (I. Kleiner and V. Ilyushin) would like to thank the “BQR” of University Paris 12 for having invited Dr. Ilyushin. This work was also done under the PEP-NEI Réseaux Formation Recherche from the French MENESR France-Ukraine-Hungary network which is also acknowledged. We acknowledge funding support from the Spanish MEC through grants AYA2006-14876 and ESP2004-665, and from the PRICIT CM project S-0505/ESP-0237 (ASTROCAM).

## References

- Bauder, A. 1979, J. Phys. Chem. Ref. Data, 8, 583
- Blake, G. A., Sutton, E. C., Masson, C. R., & Phillips, T. H. 1987, ApJ, 315, 621
- Blake, G. A., Mundy, L. G., Carlstrom, J. E., et al. 1996, ApJ, 472, L49
- Bottinelli, S., Ceccarelli, C., Williams, J. P., & Lefloch, B. 2007, A&A, 463, 601
- Bottinelli, S., Ceccarelli, C., Neri, R. 2004, ApJ, 617, L69

- Brown, R. D., Crofts, J. G., Gardner, F. F., et al. 1975, *ApJ*, 197, L29
- Carvajal, M., Willaert, F., Demaison, J., & Kleiner, I. 2007, *J. Mol. Spectrosc.*, 246, 158
- Cernicharo 1985, Internal IRAM report (Granada: IRAM)
- Churchwell, E., & Winnewisser, G. 1975, *A&A*, 45, 229
- Curl, R. F. 1959, *J. Chem. Phys.*, 30, 1529
- Demaison, J., Boucher, D., Dubrulle, A., & Van Eijck, B.P. 1983, *J. Mol. Spectrosc.*, 102, 260
- Demyk, K., Mäder, H., Tercero, B., et al. 2007, *A&A*, 466, 255
- Demyk, K., Włodarczyk, G., & Carvajal, M. 2008, *A&A*, 489, 589
- Groner, P. 1992, *J. Mol. Spectrosc.*, 156, 164
- Groner, P. 1997, *J. Chem. Phys.*, 107, 4483
- Groner, P., Albert, S., Herbst, E., & De Lucia, F. C. 1998, *ApJ*, 500, 1059
- Herbst, E., Messer, J. K., De Lucia, F. C., & Helminger, P. 1984, *J. Mol. Spectrosc.*, 108, 42
- Hollis, J. M., Lovas, F. J., & Remijan, A.J., et al. 2006, *ApJ*, 643, L25
- Horn, A., Møllendal, H., Sekiguchi, O., et al. 2004, *ApJ*, 611, 605
- Hougen, J. T., Kleiner, I., & Godefroid, M. 1994, *J. Mol. Spectrosc.*, 163, 559
- Ikeda, M., Ohishi, M., Nummelin, A., et al. 2001, *ApJ*, 560, 792
- Ilyushin, V., Alekseev, E. A., Dyubko, S. F., & Kleiner, I. 2003, *J. Mol. Spectrosc.*, 220, 170
- Ilyushin, V., Kleiner, I., & Lovas, F. J. 2008, *J. Phys. Chem. Ref. Data*, 37, 97
- Ilyushin, V., Kryvda, A., & Alekseev, E. 2009, *J. Mol. Spectrosc.*, 255, 32
- Johansson, L. E. B., Andersson, C., Elldér, J., et al. 1984, *A&A*, 130, 227
- Karakawa, Y., Oka, K., Odashima, H., Takagi, K., & Tsunekawa, S. 2001, *J. Mol. Spectrosc.*, 210, 196
- Kirtman, B. 1962, *J. Chem. Phys.*, 37, 2516
- Kleiner, I., Lovas, F. J., & Godefroid, M. 1996a, *J. Phys. Chem. Ref. Data*, 25, 1113
- Kleiner, I., Hougen, J. T., Grabow, J. U., et al. 1996b, *J. Mol. Spectrosc.*, 179, 41
- Kobayashi, K., Ogata, K., Tsunekawa, S., & Takano, S. 2007, *ApJ*, 657, L17
- Lees R. M., & Baker, J. G. 1968, *J. Chem. Phys.*, 48, 5299
- Lin C. C., & Swalen, J. D. 1959, *Rev. Mod. Phys.*, 31, 841
- Lovas, F. J. 2004, NIST Recommended rest frequencies for observed interstellar molecular microwave transitions, Gaithersburg, NIST. <http://physics.nist.gov/cgi-bin/micro/table5/start.pl>
- Maeda, A., Medvedev, I. R., De Lucia, F. C., & Herbst, E. 2008a, *Ap&SS*, 175, 138
- Maeda, A., De Lucia, F. C., & Herbst, E. 2008b, *J. Mol. Spectrosc.*, 251, 293
- Margulès, L., Motiyenko, R., Demyk, K., et al. 2009, *A&A*, 493, 565
- Margulès, L., Coudert, L. H., Møllendal, H., et al. 2009, *J. Mol. Spectrosc.*, 254, 55
- Møllendal, H., Leonov, A., & de Meijere, A. 2005, *J. Phys. Chem. A*, 109, 6344
- Møllendal, H., Cole, G. C., & Guillemin, J.-C. 2006, *J. Phys. Chem. A*, 110, 921
- Morris, M., Palmer, P., & Zuckerman, B. 1980 *ApJ*, 237, 1
- Odashima, H., Ogata, K., Takagi, K., & Tsunekawa, S. 2003, *Molecules*, 8, 139
- Oesterling, L. C., Ferguson, D. W., Herbst, E., & De Lucia, F. C. 1995, *J. Mol. Spectrosc.*, 172, 469
- Oesterling, L. C., Albert, S., De Lucia, F. C., Sastry, K. V. L. N., & Herbst, E. 1999, *ApJ*, 521, 255
- Ogata, K., Odashima, H., Takagi, K., & Tsunekawa, S. 2004, *J. Mol. Spectrosc.*, 225, 14
- Pardo, J. R., Cernicharo, J., & Serabyn, E. 2001, *IEEE Tras. Antennas and Propagation*, 49, 12
- Plummer, G. M., Blake, G. A., Herbst, E., & De Lucia, F. C. 1984, *ApJS*, 55, 633
- Plummer, G. M., Herbst, E., De Lucia, F. C., & Blake, G. A. 1986, *ApJS*, 60, 949
- Remijan, A., Shiao, Y.-S., Friedel, D. N., Meier, D. S., & Snyder, L. E. 2004, *ApJ*, 617, 384
- Senent, M. L., Villa, M., Meléndez, F. J., & Domínguez-Gómez, R. 2005, *ApJ*, 627, 567
- Uchimarui, T., Tsuzuki, S., Sugie, M., & Sekiya, A. 2003, *Chem. Phys. Lett.*, 373, 182
- Willaert, F., Møllendal, H., Alekseev, E., et al. 2006, *J. Mol. Struct.*, 795, 4